Volume 23, No 2 | International Journal of Radiation Research, April 2025

Correlation identification between radiotracer uptake and pathological features in non-small cell lung cancer (NSCLC)

Y. Sheng* and R. Zhou

Pulmonary and Critical Care Medicine, Affiliated Jinhua Hospital, Zhejiang University School of Medicine, Zhejiang, China

► ***Original article***

Corresponding author:
Yijun Sheng, M.D.,
E-mail: *zjjhsyj@163.com*

Received: January 2024
Final revised: July 2024
Accepted: August 2024

Int. J. Radiat. Res., April 2025; 23(2): 317-327

DOI: 10.61186/ijrr.23.2.317

Keywords: *Non-small cell lung cancer (NSCLC); neoplasm histological type; 18F-FDG; area under curves (AUC); diagnose.*

ABSTRACT

Background*:** SUV values from PET/CT can reflect disease progression; however, there are few detailed and comprehensive studies. In this study, we hope to provide data to complement the analysis of diagnostic indicators for NSCLC, LUAD, and LUSC by analyzing the correlation between SUVmax and various pathological parameters. ***Patients and Methods: Patients (n=298) with lung lesions were retrospectively studied and clinicopathological index of these patients were collected. Radiomics texture features were extracted by PET/CT scanning and histological features of each patient was collected. The values of SUVmax were obtained and the inner correlation was analyzed. Evaluation and scoring were performed by calculating area under the curve (AUC), sensitivity, specificity and accuracy. ***Results:*** PET data were counted and analyzed for positive/negative relationship between SUV value and T stage and histology ($P<0.05$). Mean SUVmax was 13.32±6.41 mm; the SUVmax was 14.01±5.72 for male and 11.19±7.95 for female. The results showed that LUSC tumors were smaller and more homogeneous, but with more uptake and greater PET variability. In contrast, LUAD have lower and weaker uptake, variability and homogeneity. ***Conclusion:*** By meticulously grouping nearly 300 NSCLC samples, AUC values were calculated to indicate the diagnostic value in NSCLC, LUAD and LUSC. It provides ideas and basis for pathological staging analysis of NSCLC.

INTRODUCTION

Lung cancer ranks among the TOP5 global tumor mortality rates, with NSCLC in particular being the most prevalent, accounting for roughly four-fifths of lung cancers [1-5]. By histological features, lung squamous cell carcinoma (LUSC) and lung adenocarcinoma (LUAD) were two subtype, but the prognosis and recurrence rates of these two are very different [6, 7]. Therefore, accurate diagnosis is not only meaningful for improving the treatment effect, but also for avoiding unnecessary side effects.

Nowadays, conventional morphological imaging or laboratory indicators have made us increasingly clear about the evolution of diseases, but it is equally important to analyze the changes *in vivo* through non-invasive, specific molecular imaging methods to learn biochemical information [8-10]. CT or PET/CT is often the first-line imaging method for many diseases such as tumors and is the primary source of baseline data for most NSCLC [11]. In NSCLC, FDG (18F-fluoro-2-deoxy-D-glucose) PET/CT (positron emission tomography/computed tomography) has been proved powerful means for staging judgement and efficacy assessment in last decade [12, 13]. Metrics like metabolic tumor volume (MTV) and total disease glycolysis (TLG) derived from PET/CT imaging [18F] FDG uptake have been reported and confirmed to be important in the study of metabolic activity of NSCLC [14, 15]. Other studies have demonstrated that the use of quantitative CT images to describe gene expression data enables prediction of NSCLC survival [16, 17]. More and more aspects of radiomics, including benign and malignant analysis, prognosis prediction, and metastasis, are showing potential, suggesting the prospect of personalized treatment of tumors [18-22].

The present study aims to investigate the correlation between pathological indicators and SUV values in NSCLC patients through 18F-FDG PET/CT results. How clinicopathology of lung adenocarcinoma and squamous lung cancer can be organically combined with SUV and be effectively utilized in diagnosis and efficacy is what we have been trying to reveal. In this study, the mean and median values of SUVmax, 40% SUVmax, 50% SUVmax, 60% SUVmax, and 70% SUVmax were firstly finely calculated in nearly 300 NSCLC samples apparently ingested. Secondly, meticulous grouping was performed to calculate whether the clinicopathological indicators had diagnostic value in NSCLC, LUAD and LUSC one by one, i.e., AUC values were counted. This was not available in previous studies. In addition, the correlation between SUV and prognosis was analyzed, which provided ideas and basis for pathological staging analysis of NSCLC.

[Downloaded from ijrr.com on 2026-05-26]

MATERIALS AND METHODS

Patient cohort and data collection

All enrolled patients were screened who underwent FDG PET/CT at Affiliated Jinhua Hospital, Zhejiang University School of Medicine for characterization or staging a suspected lung tumor (from 2021.05 to 2022.12). A PET/CT scans (before any treatment) baseline has been evaluated and all scans were performed. Inclusion criteria: a) >18 years; b) Presence of a single lung lesion recognisable by both CT and PET; c) a histologically confirmed diagnosis of NSCLC. Exclusion criteria: a) Unknown diagnosis due to tumor tissue too small, or inaccurate diagnosis due to sampling errors; b) Non-malignant tumors; c) FDG uptake below or approximating background activity in healthy lung parenchyma. Available clinical parameters of enrolled samples, including gender, age, smoking history, T stage, lymphatic metastasis, histological type and PET/CT characterizations, were recorded.

Histological types of NSCLC

Tumor histopathology was obtained from each patient by endobronchial ultrasound biopsy or thoracotomy. Histopathological examination was performed according to institutional standards: tumours were classified as LUAD and LUSC based on hematoxylin and eosin (HE) staining. The current WHO/IARC diagnostic criteria were adopted. Staging was conducted according to the VIIth edition TNM classification of malignant tumors. 137 patients were LUAD and 131 were LUSC; small cell carcinoma: 22, large cell carcinoma: 1 and not otherwise specified: 7. This was a retrospective study and all subjects included signed a written informed consent. Ethics approval number: [2021 Ethical Review No. (312)] was obtained from the Ethics Committee of Affiliated Jinhua Hospital.

PET/CT image acquisition

As reported by Boellaard *et al*., the patients should be positioned supine and raise his or her arms above the head as far as tolerable [23]. This means that beam -hardening artefacts in the abdominal and pelvic regions can be avoided, as well as artefacts caused by truncation of the measurement area. The CT scan is performed from the top of the head to the mid-thighs, and the PET acquisition is performed afterwards. The PET scan extends from the mid-thigh to the head. PET covers the same area as a CT scan. PET data and CT data were acquired during shallow breathing and during the baseline respiratory period, respectively. Before receiving ^{18}F-FDG (29702-43, Bayer Healthcare, Germany), patients were well-hydrated. Patients were asked to fast (blood glucose level: 150 mg/dL) 6-8 hours prior to ^{18}F-FDG PET/CT imaging and were imaged with 4 MBq/kg ^{18}F-FDG administered intravenously over approximately 60±5 minutes. PET/CT scanning were obtained by commercial PET/CT scanner (Biograph mCT-S (64); SIEMENS, Germany) after tracer injection for sixty minutes. The detailed parameters of PET/CT scanner used are listed in table 1.

Table 1. Detailed specifications of the Biograph Vision PET/CT system.

	Biograph Vision
Detector material	LSO
Detector element dimension (mm^3)	3.2×3.2 x 20
Detector elements per block	16×16
Total number of detector elements	60,800
Signal readout	SiPM (2×2 per block)
Axial field-of-view (mm)	263
Transaxial field-of-view (mm)	780
Plane spacing (mm)	1.65
Image planes	119
Coincidence time window (ns)	4.7
Energy window (keV)	435-585
Energy resolution (%)	9
System time resolution (ps)	210
NEMA sensitivity (kcps/MBq)	16.4

Image reconstruction

PET scanning: 4 mins/bed, 6-8 beds/patient (rely on height). The raw CT data were reconstructed into 3.75 mm transverse slices, on the basis of which sagittal and coronal CT images were obtained. The PET/CT analyses were interpreted by two nuclear medicine physicians (random order and independent review), and they all have more than a decade of experience in PET/CT interpretation. All data for patients other than those with suspected NSCLC were not relevant for interpretation. The review committee first analyzed the PET-sole dataset without looking at CT images and then analyzed the PET/CT dataset in following order. After each PET and PET/CT analysis, TNM staging was divided on the basis of consensus within the committee. If no clear distinction could be made between the two stages (T, N, or M), both stages were recorded and considered equivocal.

SUVmax analysis

^{18}F-FDG PET/CT positive lesions were obtained by outlining region of interest (ROI) along the lesion periphery (avoiding the area of radioactive defects such as hemorrhage and necrosis within the lesion) and then automatically calculating the lesion by the computer and obtaining the standardized uptake value (SUV). The calculation formula of SUV is radioactivity per unit volume of lesion tissue / (amount of developer injection / weight of patient). ^{18}F-FDG uptake were evaluated using SUVmax according to the scanning criteria, which determined and evaluated systematically the metabolic activity of Lymph nodes. SUVmax means the maximum standardized uptake value when scanning was performed; a quantitative indicator of radioactive uptake in a lesion. SUVmax was equivalent to developer activity rate per unit volume of lesion tissue to the amount of developer injected. Static

[Downloaded from ijrr.com on 2026-05-26]

emission scans were acquired with maximum standardized uptake values and weight corrections (for dead time, scattering and attenuation, and attenuation corrections by unenhanced low dose) calculated by the same software. A threshold of 2.5 for SUVmax is considered to allow efficient and specific detection of lesions.

Statistical analysis

All analyses in this study were done with the help of SPSS software (version 26.0, SPSS Inc, Chicago, IL, USA): the unpaired Student's t-test (two-tailed probability) and the Wilcoxon rank sum test were carried out using for means comparisons. ROC analysis, which were used to differentiate between groups at high risk of developing end-points, were employed to perform the best critical value estimation for SUVmax. Multivariate binary logistic regression analysis was employed to analyses the relationship between multiple independent variables and the dependent variable, with selected independent variables. *P* value < 0.05 was considered statistically significant.

RESULTS

Patient characteristics

Table 2 summarizes the basic information and NSCLC pathological features included in this retrospective study. Specifically, it includes: (1) The ratio of male to female in the samples collected is about 3: 1 (212: 86). (2) The sample size of patients with LUSC and LUAD was basically the same (LUAD: LUSC=137:131); The other 30 samples were small cell carcinoma: 22 (7.38%), large cell carcinoma: 1 (0.34%) and not otherwise specified: 7 (2.35%). (3) Among these 298 samples, the samples of T1/T2/T3/T4 stages was 95 (31.88%), 75 (25.17%), 45 (15.10%) and 83 (27.85%), the samples in N0/N1/N2/N3 stage was 110 (36.91%), 34 (11.42%), 76 (25.50%) and 78 (26.17%). (4) In addition, the percentage profile of smoking history was: current: 132 (44.30%); former: 30 (10.06%); never: 136 (45.64%).

PET/CT image acquisition

Two hundred and ninety-eight conventional (non-contrast-enhanced) baseline CT scans of NSCLC were included in this study. Two representative scanning sample was shown in figure 1 and figure 2. The imaging diagnosis of the patient in figure 1 was: there was an irregular soft tissue mass of about 4.3×3.9 cm in the left hilum with an SUVmax of 14.8. It was accompanied by bronchial obstruction in upper lobe of left lung; lamellar soft tissue shadows and multiple patchy increased density shadows in the upper left lung, with SUVmax of 13.0 and 2.3, respectively (figure 1A). Increased transparency of both lungs, irregular soft tissue mass in the left hilum, patchy soft tissue shadow in upper lobe of left lung, accompanied by bronchial obstruction in upper lobe of left lung. Multiple patchy increased density shadows were observed in upper lobe of left lung, and multiple small nodular shadows were observed in the right lung (figure 1B-1C). The imaging diagnosis of the patient in figure 2 was: there was an irregular soft tissue mass in inferior lobe of left lung with a size of 7.6*6.3 cm, SUVmax: 18.8. With distal strip and patchy high-density shadows, the demarcation between the lesion and the adjacent tissue is unclear. In addition, multiple enlarged lymph nodes were seen in the left hilum and mediastinum (group 5 and 7), with an SUVmax of 13.5, and multiple nodular thickenings in the left pleura with an SUVmax of 8.5 (figure 2A). Mild breast imaging on both sides, roughly symmetrical on both sides, increased uptake of strip-like imaging agent in the lower esophagus, and no abnormal imaging agent concentration in other parts of the lungs (figure 2B-2C).

Table 2. The tumor and patient characteristics.

Characteristic	Value
Age (range) years	64.81±10.60 (27-86)
Gender, n(%)	
Male	212 (71.14%)
Female	86 (28.86%)
T Stage, n(%)	
T1	95 (31.88%)
T2	75 (25.17%)
T3	45 (15.10%)
T4	83 (27.85%)
N Stage, n(%)	
N0/Nx	110 (36.91%)
N1	34 (11.42%)
N2	76 (25.50%)
N3	78 (26.17%)
Smoking History, n(%)	
Current	132 (44.30%)
Former	30 (10.06%)
Never	136 (45.64%)
Histology, n(%)	
Adenocarcinoma	137 (45.97%)
Squamous cell carcinoma	131 (43.96%)
Small cell carcinoma	22 (7.38%)
Large cell carcinoma	1 (0.34%)
Not otherwise specified	7 (2.35%)

Note: T1: T1 stage; T2: T2 stage; T3: T3 stage; T4: T4 stage; N0/Nx: N0/Nx stage; N1: N1 stage; N2: N2 stage; N3: N3 stage

Prediction and discriminating values of SUVmax

In this study, the SUVmax was reported higher than 2.5 (i.e. significant uptake) in 296 patients by PET/CT, and only two patients reported a SUVmax of less than 2.5 as measured by PET/CT. For PET features, the mean value and median value of SUVmax, 40% SUVmax, 50% SUVmax, 60% SUVmax and 70% SUVmax were calculated. The specific mean value were 12.31 ± 7.11, 4.92 ± 2.84, 6.16 ± 3.55, 7.39 ± 4.27 and 8.62 ± 4.98, respectively; the specific median value were 11.20 (range: 0-41), 4.48 (range: 0-16.4), 5.60 (range: 0-20.5), 6.72 (range: 0-24.6) and 7.84 (range: 0-28.7), respectively (table 3).

[Downloaded from ijrr.com on 2026-05-26]

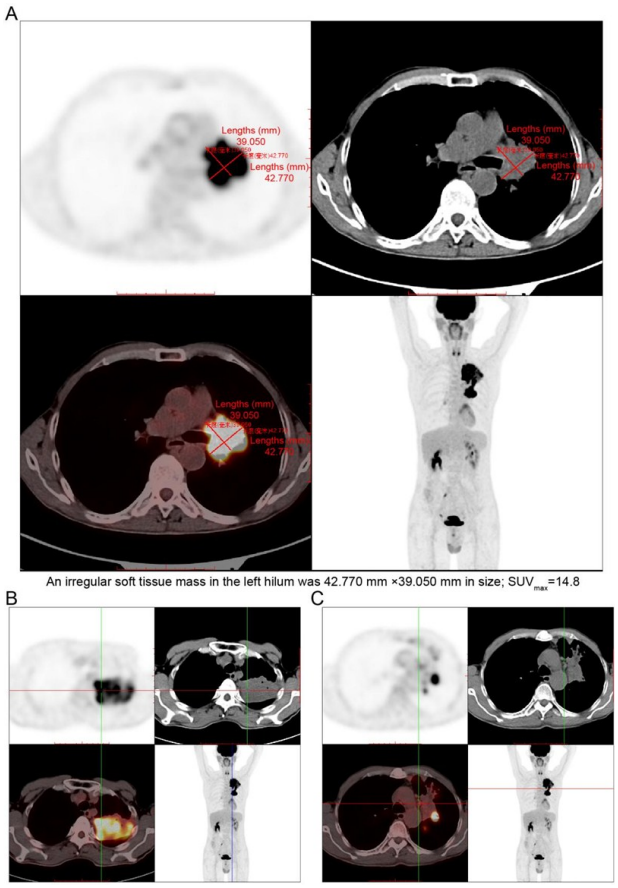

Figure 1. Computed tomographic slices from a patient with non-small-cell lung cancer. **A.** An irregular soft tissue mass in the hilum of the left lung, 4.3×3.9 cm in size; SUVmax: 14.8; **B-C.** Increased transparency of both lungs, irregular soft tissue mass in the left hilum, patchy soft tissue shadow in the upper lobe of the left lung, accompanied by bronchial obstruction in the upper lobe of the left lung. Multiple patchy increased density shadows were observed in the upper lobe of the left lung, and multiple small nodular shadows were observed in the right lung.

Table 3. Intra-modality correlation between PET features.

	Mean±SD	Median, range
SUVmax	12.31±7.11	11.20, 0-41
40%SUVmax	4.92±2.84	4.48, 0-16.4
50%SUVmax	6.16±3.55	5.60, 0-20.5
60%SUVmax	7.39±4.27	6.72, 0-24.6
70%SUVmax	8.62±4.98	7.84, 0-28.7

Correlation between clinical characteristics and SUVmax

The low SUVmax and high SUVmax groups were grouped according to the median SUVmax; and univariate analysis and multivariate analysis were performed, subsequently. The univariate analysis revealed that age (95% CI: 0.043-0.139; OR=0.078; *P*<0.01) and gender (95% CI: 0.080-0.555; OR=0.211; *P*<0.01) were different between low SUVmax group and high SUVmax group (table 4). The results of the multivariate analysis showed that differences in smoking history (95% CI: 0.053-0.486; OR=0.161; *P*<0.01), T stage (95% CI: 1.980-114.220; OR=15.039; *P*<0.01) N stage (95% CI: 3.846-75.143; OR=17.000; *P*<0.01), and histology features (95% CI: 1.604-19.849; OR=5.642; *P*<0.01) between low SUVmax group and high SUVmax group (table 4). In addition, to further confirm whether T stage, N stage and smoking history was associated with histological characteristics (LUAD or LUSC) according to SUVmax value, we performed the following statistical analysis (table 5). The analysis revealed that in LUAD, high SUVmax group and low SUVmax group presented differences on age (*P*<0.01), T stage (*P*<0.01) and N stage (*P*<0.01), respectively. In contrast, in LUSC, only age (*P*<0.01) differed between high SUVmax group and low SUVmax group (table 5).

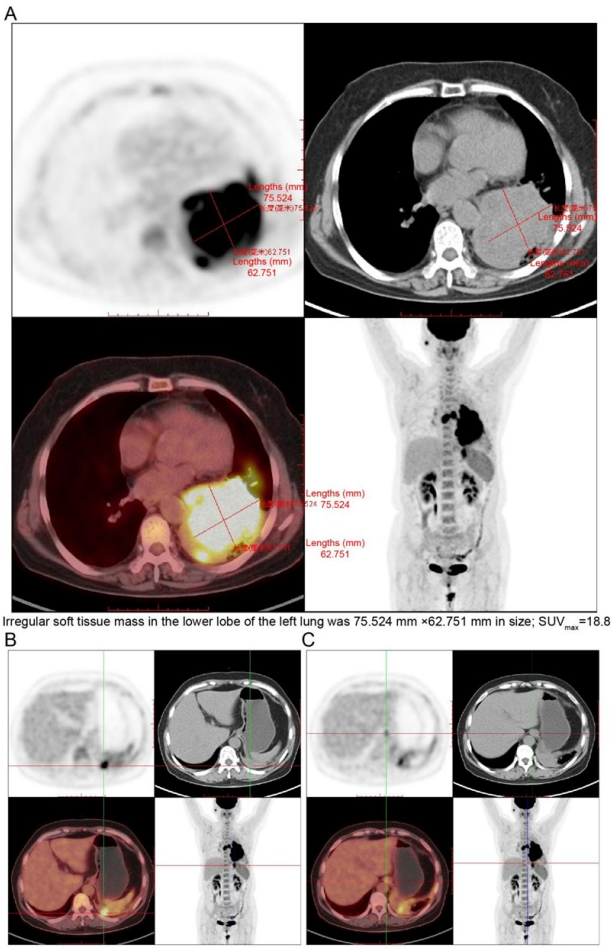

Figure 2. Computed tomographic slices from a patient with non-small-cell lung cancer. **A.** An irregular soft tissue mass in the lower lobe of the left lung, size 7.6*6.3 cm, SUVmax: 18.8; **B-C.** Mild breast imaging on both sides, roughly symmetrical on both sides, increased uptake of strip like imaging agent in the lower esophagus, and no abnormal imaging agent concentration in other parts of the lungs.

ROC curve analysis of SUVmax by pathological features

According to the above analysis, the median value of SUVmax was used as the cut off for gender, age, smoking history, TNM stage and histology grouping based on the results analysed above. The ROC curve analysis revealed that significant difference was calculated in four indexes: gender, smoking history, T

[Downloaded from ijrr.com on 2026-05-26]

stage and histology feature (p<0.01, figure 3, D, F, J and L); AUC were 0.673, 0.666, 0.632 and 0.718, respectively. Also, the ROC curve analysis of age showed that the AUC were 0.573 and the difference is significant (p<0.05, figure 3E). The ROC curve analysis in N stage have no significant difference, and the AUC were 0.603, respectively (figure 3K). The distribution of SUVmax in each subgroup was shown in the figure 3A-C, 3G-I. The median value of SUVmax was used as the cut off for gender, age, smoking history, TNM stage grouping based on the results analysed above in LUSC. The ROC curve analysis revealed that the AUC were 0.627, 0.558, 0.527, 0.563 and 0.598, respectively (figure 4D-F, 4I and J); no significant difference was found in these indexes. The distribution of SUVmax in each subgroup was shown in the figure 4A-C, 4G-H. The median value of SUVmax was used as the cut off for gender, age, smoking history, TNM stage grouping based on the results analyzed above in LUAD. The ROC curve analysis revealed that there was a significant difference in T stage and its AUC value was 0.641 (p<0.01, figure 5I). The ROC curve analysis in other four indexes showed no significant difference and AUC value were 0.592, 0.559, 0.606 and 0.595, respectively (figure 5D-F, 5J). Besides, the distribution of SUVmax in each subgroup was shown in the figure 5A-C, 5G-H.

Table 4. Logistic regression analysis.

		Age (mean)	Gender (M/F)	Smoking History (C/F/N)	T Stage (1/2/3/4)	N Stage (0/1/2/3)	Histology (A/S/Not)
Low SUVmax Group		57.42±9.19	7/12	4/0/15	17/1/0/1	17/2/0/0	16/3/0
High SUVmax Group		65.32±14.02	205/74	128/30/121	78/74/45/82	93/34/74/78	121/128/7
Uni-analysis	OR	0.078	0.211	-	-	-	-
	95% CI	0.043-0.139	0.080-0.555	-	-	-	-
	P	0.000**	0.001**	-	-	-	-
Multi-analysis	OR	-	-	0.161	15.039	17.000	5.642
	95% CI	-	-	0.053-0.486	1.980-114.220	3.846-75.143	1.604-19.849
	P	-	-	0.000**	0.001**	0.000**	0.003**

Note: M: Male; F: Female; C: Current; F: Former; N: Never; 0: N0 stage; 1: T1 stage/N1 stage; 2: T2 stage/N2 stage; 3: T3 stage/N3 stage; 4: T4 stage; A: Adenocarcinoma; S: Squamous cell carcinoma; Not: Not otherwise specified; Uni-analysis: Univariate analysis; Multi-analysis: Multivariate analysis.

Table 5. The results of correlation and regression analysis.

	LUAD		LUSC	
Items	Low Group vs. High Group n (%)	x^2/P	Low Group vs. High Group n (%)	x^2/P
Age (mean)	54.81±7.16; 64.65±11.32	37.322/0.000**	71.33±14.19; 65.18±7.73	82.987/0.000**
Gender		2.796/0.094		0.122/0.727
Male	4 (25.00%); 57 (47.11%)		3 (100%); 123 (96.09%)	
Female	12 (75.00%); 64 (52.89%)		0 (0%); 5 (3.91%)	
Smoking		1.194/0.550		0.992/0.609
Current	2 (12.50%); 23 (19.01%)		2 (66.67%); 86 (67.18%)	
Former	0 (0%); 5 (4.13%)		0 (0%); 21 (16.41%)	
Never	14 (87.50%); 93 (76.86%)		1 (33.33%); 21 (16.41%)	
T Stage		21.279/0.000**		0.860/0.835
T1	16 (100%); 47 (38.84%)		1 (33.33%); 28 (21.88%)	
T2	0 (0%); 19 (15.70%)		1 (33.33%); 44 (34.38%)	
T3	0 (0%); 14 (11.57%)		0 (0%); 25 (19.53%)	
T4	0 (0%); 41 (33.88%)		1 (33.33%); 31 (24.22%)	
N Stage		20.663/0.000**		2.032/0.566
N0	16 (100%); 48 (39.67%)		1 (33.33%); 42 (32.81%)	
N1	0 (0%); 12 (9.92%)		0 (0%); 17 (13.28%)	
N2	0 (0%); 18 (14.88%)		2 (66.67%); 42 (32.81%)	
N3	0 (0%); 43 (35.54%)		0 (0%); 27 (21.09%)	

Note: LUAD: Adenocarcinoma; LUSC: Squamous cell carcinoma; SCLC: small cell lung cancer; LCLC: Large cell lung cancer; Not: Not otherwise specified.

Table 4. Logistic regression analysis.

		Age (mean)	Gender (M/F)	Smoking History (C/F/N)	T Stage (1/2/3/4)	N Stage (0/1/2/3)	Histology (A/S/Not)
Low SUVmax Group		57.42±9.19	7/12	4/0/15	17/1/0/1	17/2/0/0	16/3/0
High SUVmax Group		65.32±14.02	205/74	128/30/121	78/74/45/82	93/34/74/78	121/128/7
Uni-analysis	OR	0.078	0.211	-	-	-	-
	95% CI	0.043-0.139	0.080-0.555	-	-	-	-
	P	0.000**	0.001**	-	-	-	-
Multi-analysis	OR	-	-	0.161	15.039	17.000	5.642
	95% CI	-	-	0.053-0.486	1.980-114.220	3.846-75.143	1.604-19.849
	P	-	-	0.000**	0.001**	0.000**	0.003**

Note: LUAD: Adenocarcinoma; LUSC: Squamous cell carcinoma; SCLC: small cell lung cancer; LCLC: Large cell lung cancer; Not: Not otherwise specified.

[Downloaded from ijrr.com on 2026-05-26]

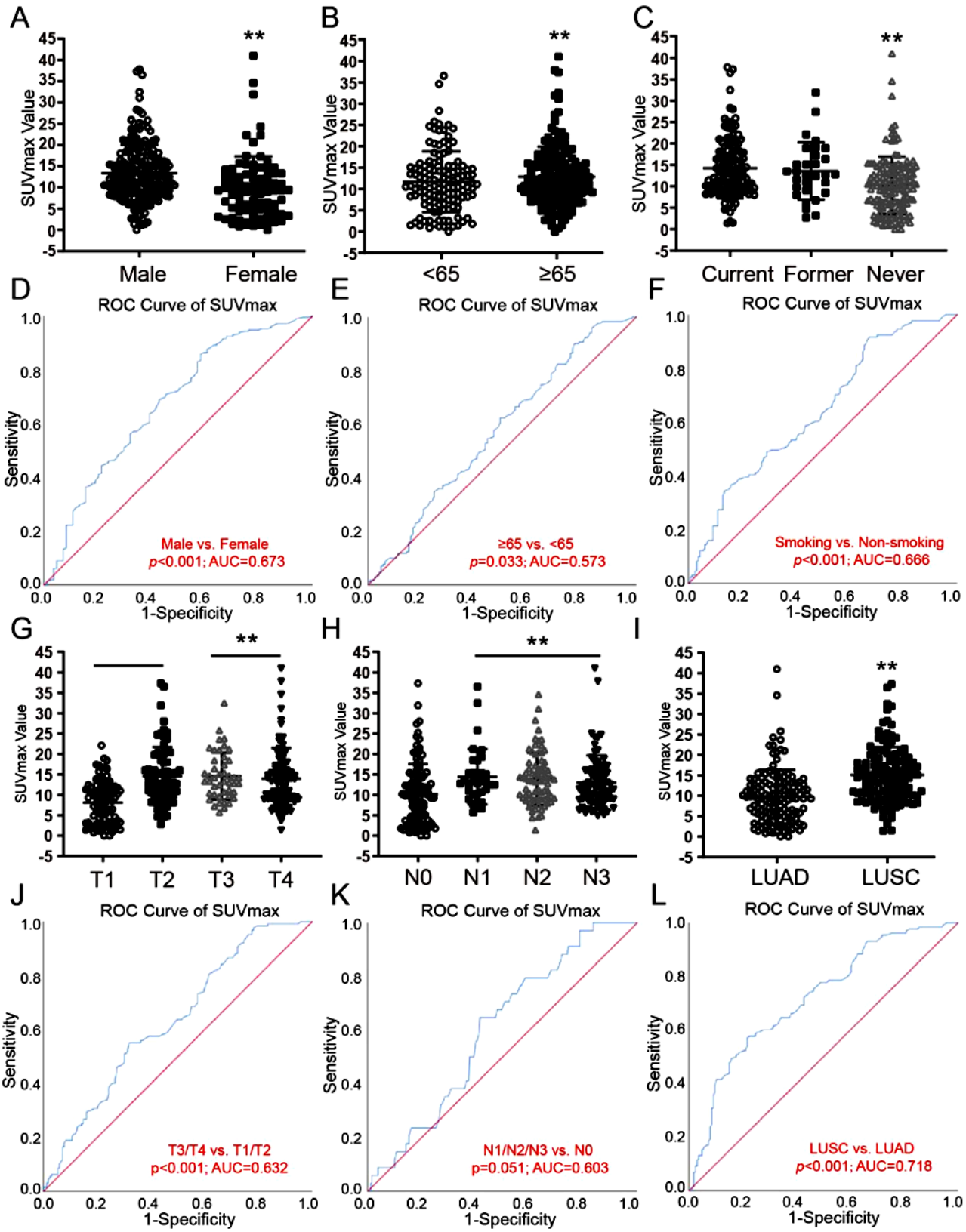

Figure 3. ROC curve analysis establishing the cut off value of SUVmax. **(A&D)** The distribution and ROC curve of SUVmax in male and female; **(B&E)** The distribution and ROC curve of SUVmax in <65 years and ≥ 65 years; **(C&F)** The distribution and ROC curve of SUVmax in current smoker, former smoker and never smoker; **(G&J)** The distribution and ROC curve of SUVmax in T1/T2/T3/T4; **(H&K)** The distribution and ROC curve of SUVmax in N0/N1/N2/N3; **(I&L)** The distribution and ROC curve of SUVmax in LUAD and LUSC.

[Downloaded from ijrr.com on 2026-05-26]

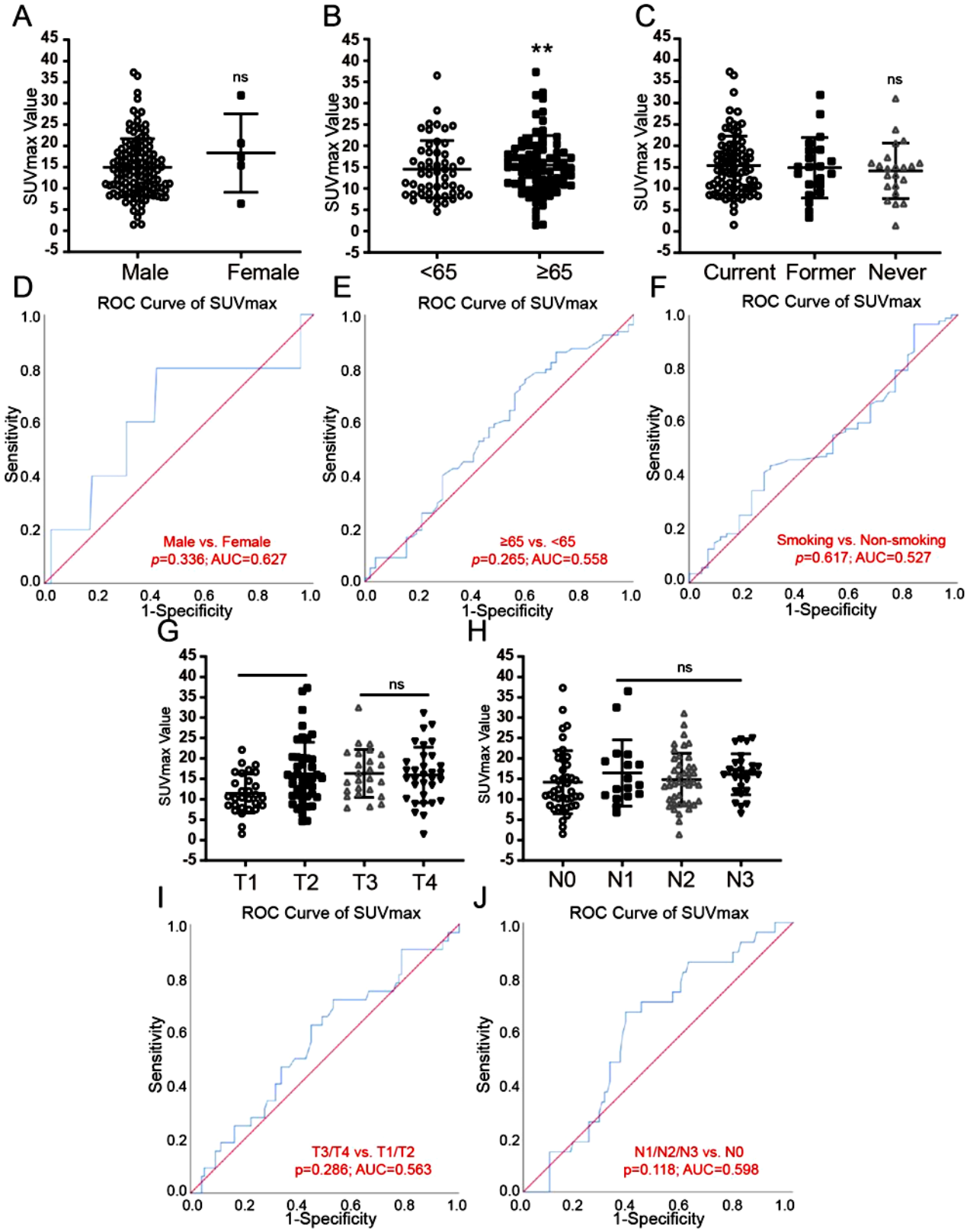

Figure 4. ROC curve analysis establishing the cut off value of SUVmax in LUSC. **(A&D)** The distribution and ROC curve of SUVmax in male and female; **(B&E)** The distribution and ROC curve of SUVmax in <65 years and ≥ 65 years; **(C&F)** The distribution and ROC curve of SUVmax in current smoker, former smoker and never smoker; **(G&I)** The distribution and ROC curve of SUVmax in T1/T2/T3/T4; **(H&J)** The distribution and ROC curve of SUVmax in N0/N1/N2/N3.

[Downloaded from ijrr.com on 2026-05-26]

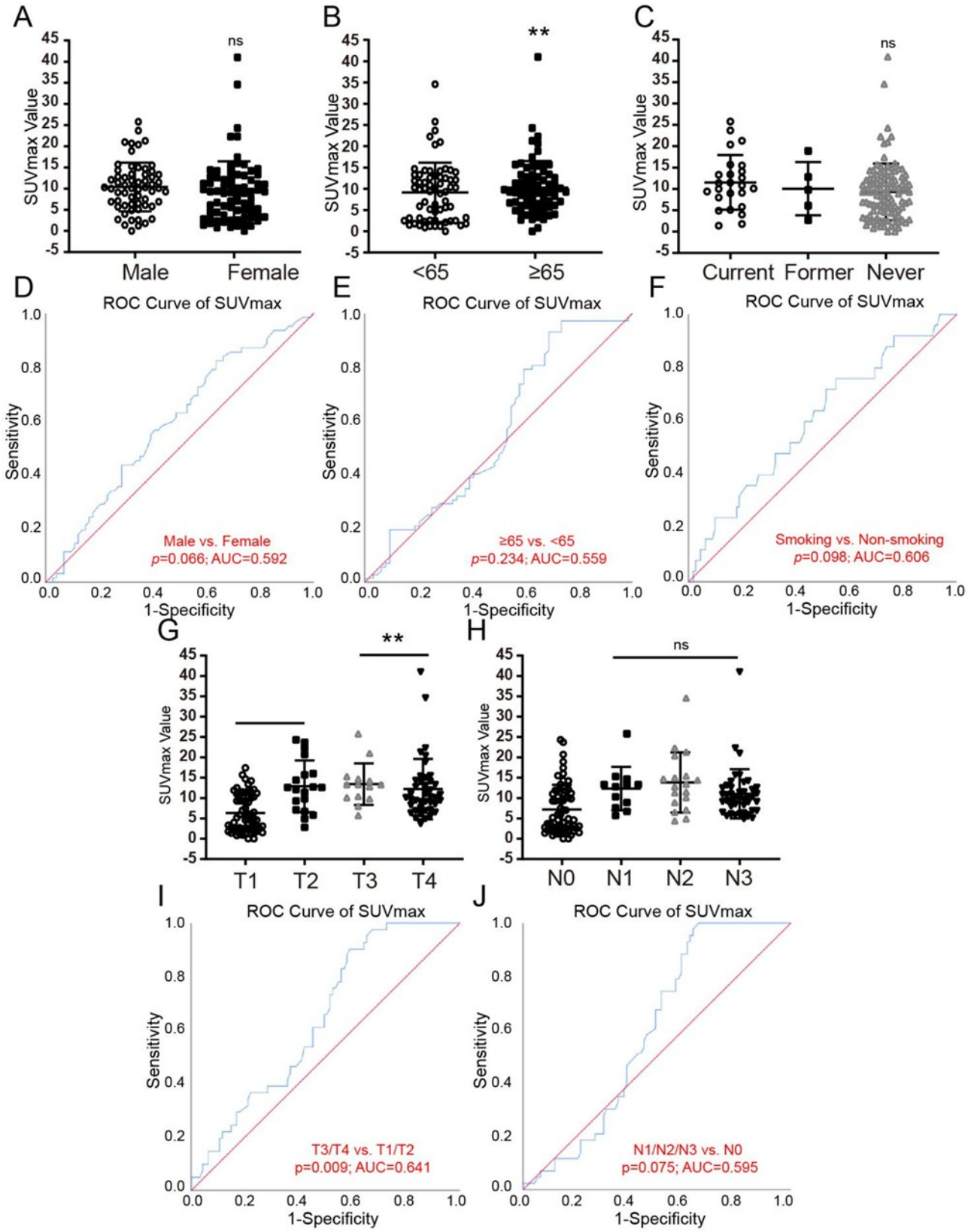

Figure 4. ROC curve analysis establishing the cut off value of SUVmax in LUSC. **(A&D)** The distribution and ROC curve of SUVmax in male and female; **(B&E)** The distribution and ROC curve of SUVmax in <65 years and ≥ 65 years; **(C&F)** The distribution and ROC curve of SUVmax in current smoker, former smoker and never smoker; **(G&I)** The distribution and ROC curve of SUVmax in T1/T2/T3/T4; **(H&J)** The distribution and ROC curve of SUVmax in N0/N1/N2/N3.

[Downloaded from ijrr.com on 2026-05-26]

Table 5. The results of correlation and regression analysis

	LUAD		LUSC	
Items	Low Group vs. High Group n (%)	x^2/P	Low Group vs. High Group n (%)	x^2/P
Age (mean)	54.81±7.16; 64.65±11.32	37.322/0.000**	71.33±14.19; 65.18±7.73	82.987/0.000**
Gender		2.796/0.094		0.122/0.727
Male	4 (25.00%); 57 (47.11%)		3 (100%); 123 (96.09%)	
Female	12 (75.00%); 64 (52.89%)		0 (0%); 5 (3.91%)	
Smoking		1.194/0.550		0.992/0.609
Current	2 (12.50%); 23 (19.01%)		2 (66.67%); 86 (67.18%)	
Former	0 (0%); 5 (4.13%)		0 (0%); 21 (16.41%)	
Never	14 (87.50%); 93 (76.86%)		1 (33.33%); 21 (16.41%)	
T Stage		21.279/0.000**		0.860/0.835
T1	16 (100%); 47 (38.84%)		1 (33.33%); 28 (21.88%)	
T2	0 (0%); 19 (15.70%)		1 (33.33%); 44 (34.38%)	
T3	0 (0%); 14 (11.57%)		0 (0%); 25 (19.53%)	
T4	0 (0%); 41 (33.88%)		1 (33.33%); 31 (24.22%)	
N Stage		20.663/0.000**		2.032/0.566
N0	16 (100%); 48 (39.67%)		1 (33.33%); 42 (32.81%)	
N1	0 (0%); 12 (9.92%)		0 (0%); 17 (13.28%)	
N2	0 (0%); 18 (14.88%)		2 (66.67%); 42 (32.81%)	
N3	0 (0%); 43 (35.54%)		0 (0%); 27 (21.09%)	

DISCUSSION

The increasing role of radiomics in clinical is nothing less than its convenient realization of non-invasive acquisition of *in vivo* lesions characteristics (including prognostic data and treatment response) [24, 25]. PET/CT has the advantage of achieving co-integration of images from both functional and anatomical morphological perspectives, but it still suffers from deficiencies such as too small lesions that cannot be identified, and poor display of anatomical structures around lesions due to tissue specificity of tracers, and difficult image comprehension [26, 27]. Thus, Biopsy is necessary for histological classification of disease. In our study, the relations between [18F] FDG PET features, CT features, and histological types have been evaluated. After nearly 300 NSCLC samples were grouped according to SUVmax, statistical analysis confirmed the correlation between age, gender and SUVmax group; and between smoking history, T stage, N stage and histological features and SUVmax group.

We know that SUVmax can reflect the degree of tumor uptake of FDG, that is, an indicator that reflects the level of tumor glucose metabolism. Metabolic volume MTV that reflects the tumor burden of solid tumors can be obtained by PET/CT imaging [28-30]. Therefore, we next used the median values of 40% SUVmax, 50% SUVmax, 60% SUVmax and 70% SUVmax to count the correlations with clinical indicators, respectively. Statistical analysis of our results revealed that SUVmax correlated with tumor clinical stage, lymph node involvement, and histological features. Previous studies have shown that patients with higher SUVmax values have a poorer prognosis compared with those with lower SUVmax values, indicating higher glycolytic activity, which predicts adverse responses to subsequent therapy [31]. Also, Pyka *et al.* uncovered that tumor heterogeneity obtained by FDG-PET texture analysis correlated with the response of NSCLC patients to radiotherapy efficacy, suggesting that imaging and correspondence analysis data can be useful for individualizing treatment and analyzing the population benefiting from different treatment options [32].

Studies have confirmed that the sensitivity, specificity, positive predictive rate and negative predictive rate of PET/CT were 96%, 92%, 92%, and 95%, respectively [33]. In our study, we combined PET/CT results and clinicopathological data and performed correlation analysis by grouping according to SUVmax values. It revealed a correlation between age, gender, smoking history, and stage with SUVmax groups in NSCLC. It also confirmed that age, T-stage and N-stage were correlated with SUVmax values in LUAD by lung adenocarcinoma or lung squamous carcinoma, while only age was correlated with SUVmax values in LUSC. Similar studies are scarce, with one similar study of only 119 cases by Christian *et al.* [34]. Our results are a strong addition to the clinical data.

LUAD and LUSC, the two main histological subtypes of NSCLC, differ in terms of prognosis and recurrence. Therefore, accurate diagnosis and follow-up can avoid unnecessary side effects [35]. Clinical patients will benefit from the combination of pathological staging and non-invasive imaging, which is used to further adjust therapeutic plans by tracking pathological progression. Therefore, our study enrolled a nearly 300 cases sample size (LUAD: LUSC close to 1:1), and try to discover the patterns and correlations and provide data support for clinical application. The median of SUVmax was used as the cutoff value for gender, age, smoking history, TNM stage, and histological grouping. ROC curve analysis revealed significant differences in four indicators: gender, smoking history, T stage, and histological

[Downloaded from ijrr.com on 2026-05-26]

characteristics. The current study is not without its limitations: on the one hand, the size of the sample, which may produce some unexpected results, and there is no systematic statistics between CT features and overall survival, which is not helpful for the analysis of survival. It is worth mentioning that, by calculating the AUC value, we carried out ROC analysis to determine the relationship between SUVmax and pathological indicators [36].

CONCLUSION

In this study, the diagnostic accuracy and correlation of SUVmax with pathological indicators of patients with NSCLC were evaluated. These data should be fully utilized and organically combined for individualized treatment and prognostic assessment. This study analyzed the diagnostic value of SUV under different subgroups, which can provide research ideas and data support for pathological staging analysis of NSCLC.

ACKNOWLEDGEMENTS

We appreciate the clinicopathological index information collected in the Department of Pulmonary and Critical Care Medicine from Affiliated Jinhua Hospital in Zhejiang University School of Medicine.

***Funding*:** This research did not receive any specific grant from funding agencies in the public, commercial, or not-for-profit sectors.

Declaration of interests: The authors have no competing interests to declare that are relevant to the content of this article.

***Ethical approval*:** This research was informed consent was reached from all patients and approved received endorsement from the Affiliated Jinhua Hospital, Zhejiang University School of medical ethics committee (the ethical approval number: [2021 Ethical Review No. (312)]).

***Author contributions*:** All authors contributed to the study conception and design. Material preparation, data collection and analysis were performed by Y.S. and R.Z. The first draft of the manuscript was written by Y.S. and all authors commented on this version of the manuscript. All authors read and approved the final manuscript.

REFERENCES

1. Bray F, Laversanne M, Sung H, *et al*. (2024) Global cancer statistics 2022: GLOBOCAN estimates of incidence and mortality worldwide for 36 cancers in 185 countries. *CA Cancer J Clin, **74**(3): 229-263*.
2. Kratzer TB, Bandi P, Freedman ND, *et al*. (2024) Lung cancer statistics, 2023. *Cancer, **130**(8): 1330-1348*.
3. Leiter A, Veluswamy RR, Wisnivesky JP (2023) The global burden of lung cancer: current status and future trends. *Nat Rev Clin Oncol, **20**(9): 624-639*.
4. Lee E and Kazerooni EA (2022) Lung cancer screening. *Semin Respir Crit Care Med, **43**(6): 839-850*.
5. Wu F, Wang L, Zhou C (2021) Lung cancer in China: current and prospect. *Curr Opin Oncol, **33**(1): 40-46*.
6. Sugai Y, Kadoya N, Tanaka S, *et al*. (2021) Impact of feature selection methods and subgroup factors on prognostic analysis with CT-based radiomics in non-small cell lung cancer patients. *Radiat Oncol, **16**(1): 80*.
7. Wang BY, Huang JY, Chen HC, *et al*. (2020) The comparison between adenocarcinoma and squamous cell carcinoma in lung cancer patients. *J Cancer Res Clin Oncol, **146**(1): 43-52*.
8. Kalemaki MS, Karantanas AH, Exarchos D, *et al.* (2020) PET/CT and PET/MRI in ophthalmic oncology (Review). *Int J Oncol, **56**(2): 417-429*.
9. Zangeneh M, Nedaei HA, Mozdarani H, *et al*. (2019) Enhanced cytotoxic and genotoxic effects of gadolinium-doped ZnO nanoparticles on irradiated lung cancer cells at megavoltage radiation energies. *Mater Sci Eng C Mater Biol Appl, **103**: 109739*.
10. Zhang X, Zhang G, Qiu X, *et al*. (2024) Exploring non-invasive precision treatment in non-small cell lung cancer patients through deep learning radiomics across imaging features and molecular phenotypes. *Biomark Res, **12**(1): 12*.
11. Schillaci O, Scimeca M, Toschi N, *et al*. (2019) Combining Diagnostic Imaging and Pathology for Improving Diagnosis and Prognosis of Cancer. *Contrast Media Mol Imaging. **2019**: 9429761*.
12. Otani T, Ikushima H, Bando Y, *et al*. (2023) Early prediction of radiotherapeutic efficacy in a mouse model of non-small cell lung carcinoma using 18F-FLT and 18F-FDG PET/CT. *J Med Invest, **70**(3.4): 361-368*.
13. Kagimoto A, Tsutani Y, Mimae T, *et al.* (2022) Segmentectomy versus lobectomy for solid predominant cN0 lung cancer: analysis using visual evaluation of positron emission tomography. *Eur J Cardiothorac Surg, **61**(2): 279-286*.
14. Cegla P, Bryl M, Witkowska K, *et al*. (2021) Differences between TNM classification and 2-[18F]FDG PET parameters of primary tumor in NSCLC patients. *Rep Pract Oncol Radiother, **26**(3): 445-450*.
15. Pirayesh E, Amoui M, Akhlaghpoor S, *et al*. (2014) Technical Considerations of Phosphorous-32 Bremsstrahlung SPECT Imaging after Radioembolization of Hepatic Tumors: A Clinical Assessment with a Review of Imaging Parameters. *Radiol Res Pract, **2014**: 407158*.
16. Lee J, Li B, Cui Y, *et al*. (2018) A quantitative CT imaging signature predicts survival and complements established prognosticators in stage I non-small cell lung cancer. *Int J Radiat Oncol Biol Phys, **102**(4): 1098-1106*.
17. Han Y, Dong Z, Xing Y, *et al*. (2023) Establishment of a prognosis prediction model for lung squamous cell carcinoma related to PET/CT: basing on immunogenic cell death-related lncRNA. *BMC Pulm Med, **23**(1): 511*.
18. Mozdarani H (2012) Biological complexities in radiation carcinogenesis and cancer radiotherapy: impact of new biological paradigms. *Genes (Basel), **3**(1): 90-114*.
19. Liang L, Zhang H, Lei H, *et al.* (2022) Diagnosis of benign and malignant pulmonary ground-glass nodules using computed tomography radiomics parameters. *Technol Cancer Res Treat, **21**: 15330338221119748*.
20. Kadoya N, Tanaka S, Kajikawa T, *et al*. (2020) Homology-based radiomic features for prediction of the prognosis of lung cancer based on CT-based radiomics. *Med Phys, **47**(5): 2197-2205*.
21. Wang R, Dai W, Gong J, *et al*. (2022) Development of a novel combined nomogram model integrating deep learning-pathomics, radiomics and immunoscore to predict postoperative outcome of colorectal cancer lung metastasis patients. *J Hematol Oncol, **15**(1): 11*.
22. Pfaehler E, Mesotten L, Zhovannik I, *et al*. (2021) Plausibility and redundancy analysis to select FDG-PET textural features in non-small cell lung cancer. *Med Phys, **48**(3): 1226-1238*.
23. Boellaard R, Delgado-Bolton R, Oyen WJ, *et al.* (2015) FDG PET/CT: EANM procedure guidelines for tumor imaging: version 2.0. *Eur J Nucl Med Mol Imaging, **42**(2): 328-54*.
24. Zhou R, Cai Z, Yuan Y, *et al*. (2024) Study on the application value of combined detection of multiple tumor markers in lung cancer classification diagnosis. *Int J Radiat Res, **22** (2): 283-287*.
25. Chetan MR and Gleeson FV (2021) Radiomics in predicting treatment response in non-small-cell lung cancer: current status, challenges and future perspectives. *Eur Radiol, **31**(2): 1049-1058*.
26. Deng J, Ren W, Shen J, *et al.* (2024) Maximum PET/CT 18F-FDG uptake of lymph nodes predict prognosis in esophageal squamous

[Downloaded from ijrr.com on 2026-05-26]

cell carcinoma. *Int J Radiat Res,* ***22*** *(2): 265-270*.
27. Pang Y, Zhao L, Meng T, *et al.* (2023) PET imaging of fibroblast activation protein in various types of cancer using ^{68}Ga-FAP-2286: Comparison with ^{18}F-FDG and ^{68}Ga-FAPI-46 in a single-center, prospective study. *J Nucl Med,* ***64****(3): 386-394*.
28. Liao S, Penney BC, Wroblewski K, *et al*. (2012) Prognostic value of metabolic tumor burden on 18F-FDG PET in nonsurgical patients with non-small cell lung cancer. *Eur J Nucl Med Mol Imaging,* ***39*** *(1): 27-38*.
29. Chen X, Shen L, Hong Y (2023) 18F-fluorodeoxyglucose positron emission tomography/computed tomography for predicting prognosis of small cell lung cancer patients. *Int J Radiat Res,* ***21****(2): 211-215*.
30. Hicks RJ. (2022) The Value of the standardized uptake value (SUV) and metabolic tumor volume (MTV) in lung cancer. *Semin Nucl Med,* ***52****(6): 734-744*.
31. Rogasch JMM, Furth C, Chibolela C, *et al*. (2020) Validation of independent prognostic value of asphericity of 18F-fluorodeoxyglucose uptake in non-small-cell lung cancer patients undergoing treatment with curative intent. *Clin Lung Cancer,* ***21*** *(3): 264-272.e6*.
32. Pyka T, Bundschuh RA, Andratschke N, *et al*. (2015) Textural features in pre-treatment [F18]-FDG-PET/CT are correlated with risk of local recurrence and disease-specific survival in early-stage NSCLC patients receiving primary stereotactic radiation therapy. *Radiat Oncol,* ***10****: 100*.
33. Mallorie A, Goldring J, Patel A, *et al*. (2017) Assessment of nodal involvement in non-small-cell lung cancer with 18F-FDG-PET/CT: mediastinal blood pool cut-off has the highest sensitivity and tumor SUVmax/2 has the highest specificity. *Nucl Med Commun,* ***38*** *(8): 715-719*.
34. Casali C, Cucca M, Rossi G, *et al.* (2010) The variation of prognostic significance of Maximum Standardized Uptake Value of [18F]-fluoro-2-deoxy-glucose positron emission tomography in different histological subtypes and pathological stages of surgically resected Non-Small Cell Lung Carcinoma. *Lung Cancer,* ***69****(2): 187-93*.
35. Zengin T and Önal-Süzek T (2021) Comprehensive profiling of genomic and transcriptomic differences between risk groups of lung adenocarcinoma and lung squamous cell carcinoma. *J Pers Med,* ***11****(2): 154*.
36. Li J, Ge S, Sang S, *et al*. (2021) Evaluation of PD-L1 expression level in patients with non-small cell lung cancer by 18F-FDG PET/CT radiomics and clinicopathological characteristics. *Front Oncol,* ***11****: 789014*.

[Downloaded from ijrr.com on 2026-05-26]

[Downloaded from ijrr.com on 2026-05-26]